ELSEVIER

NeuroImage

www.elsevier.com/locate/ynimg
NeuroImage 29 (2006) 321 – 327

Short Communication

Detection of signal synchronizations in resting-state fMRI datasets

Bertrand Thirion,* Silke Dodel, and Jean-Baptiste Poline

Service Hospitalier Frédéric Joliot, Département de Recherche Médicale-CEA-DSV, 4, Place du Général Leclerc, 91401 Orsay Cedex, France

Received 25 April 2005; revised 28 June 2005; accepted 29 June 2005
Available online 29 August 2005

In this paper, we propose a generic framework for the analysis of steady-state fMRI datasets, applied here to resting-state datasets. Our approach avoids the introduction of user-defined seed regions for the study of spontaneous activity. Unlike existing techniques, it yields a sparse representation of resting-state activity networks which can be characterized and investigated fairly easily in a semi-interactive fashion. We proceed in several steps, based on the idea that spectral coherence of the fMRI time courses in the low frequency band carries the information of interest. In particular, we address the question of building adapted representations of the data from the spectral coherence matrix. We analyze nine datasets taken from three subjects and show resting-state networks validated by EEG-fMRI simultaneous acquisition literature, with low intra-subject variability; we also discuss the merits of different (rapid/slow) fMRI acquisition schemes.

Introduction

Functional MR Imaging (fMRI) has been mainly used in detecting task-related metabolic activity related to neuronal activation. However, spontaneous signal fluctuations have also been described (Biswal et al., 1995; Cordes et al., 2001), and an important question about these fluctuations is their relationship with functional connectivity. Understanding these fluctuations may benefit activation studies that contrast a controlled activation state against the so-called resting state; the evolution of these fluctuations during learning or pathology may be particularly informative; moreover, they can characterize brain processes associated with attention and vigilance. Therefore, it is important to distinguish between different possible origins of the signal, e.g. acquisition/motion artifacts, or aliased respiratory and cardiac signals (Dodel et al., 2004), which potentially contribute to low-frequency fluctuations of the signal. A convenient way to overcome these difficulties consists in performing simultaneous acquisition of respiratory and cardiac rhythms (Dodel et al., 2004), or electro-encephalographic (EEG) activity (Goldman et al., 2002; Laufs et al., 2003). Besides the technical difficulty of these multimodal acquisition procedures, there remains the open issue of what the fMRI signal structure alone reveals about spontaneous activity.

Analysis of resting-state fMRI data

Detection of resting-state activity (RSA) is a challenging task, because the resulting signals are confounded by physiological noise and there exist only weak spatial- and frequency-domain priors on the measurement artifacts. Frequency analysis of the individual time courses seems natural, since RSA has been shown to result in prominently low-frequency contributions; for instance, the Fast Fourier Transform (FFT) has been used by Kiviniemi et al. (2000), but this approach is not very accurate spatially (Kiviniemi et al., 2004). Cross-correlation analysis (Biswal et al., 1995; Cordes et al., 2001) requires the prior definition of a reference region, biasing the description towards subjective guess. The correlation between any two regions in the brain is also sensitive to physiological (motion-related, cardiac and respiratory) signals, which may induce strong correlations, even after adequate denoizing (Dodel et al., 2004). A frequency analysis of the cross-correlations might better separate the different contributions (Cordes et al., 2001). Finally, coherence analysis with reference or seed regions has also been proposed (Sun et al., 2004).

On the other hand, multivariate analysis builds on the spatially distributed structure of RSA. Principal Components Analysis (PCA) has been introduced for the analysis of the so-called *functional connectivity* (Friston et al., 1993), but spatial Independent Components Analysis (ICA) is known to be more successful in the separation of potential sources of signal (Kiviniemi et al., 2004). However, these methods face difficult dimension estimation issues (Beckmann and Smith, 2004). Moreover, the resulting components have to be further analyzed in order to select spatial- or frequency-domain components that match prior hypotheses on RSA. For instance, the average values of these maps can be recorded in regions of interest (van de Ven et al., 2004). Finally, the spatial maps have to be thresholded, which is usually performed by ad hoc procedures (z transforms and thresholding). These difficulties limit the reliability of these methods, while the lack of prior information may weaken their sensitivity. The present work is a novel combination of univariate methods (spectral coherence) and multivariate analysis (dimension reduction and clustering).

* Corresponding author. Fax: +33 1 69 86 77 86.
E-mail address: thirion@shfj.cea.fr (B. Thirion).
Available online on ScienceDirect (www.sciencedirect.com).

1053-8119/$ - see front matter © 2005 Elsevier Inc. All rights reserved.
doi:10.1016/j.neuroimage.2005.06.054

Spectral coherence

Our approach is based on the prior knowledge that RSA results in low-frequency coherent signals. Following Müller et al. (2001), we thus start by evaluating spectral coherence of the signals across all pairs of regions (or voxels).

Let $Y(t) = [Y_1(t),\ldots,Y_N(t)]$ be the multivariate stochastic process that represents fMRI data. This process is assumed to be weakly stationary, i.e.:

$$\mathbb{E}(Y_j(t)) = m_j \tag{1}$$

$$\mathbb{E}((Y_j(t+\tau) - m_j)(Y_k(t) - m_k)) = C_{jk}(\tau) \tag{2}$$

where $\mathbb{E}(.)$; stands for the expectation operator, and τ is an arbitrary time lag. Let $C(\tau) = (C_{jk}(\tau))$ be the Cross-Correlation matrix, and assume that it has a spectral representation that admits a density f_{jk}

$$C_{jk}(\tau) = \frac{1}{2\pi}\int_{[-\pi,\pi]} e^{i\lambda\tau} f_{jk}(\lambda) d\lambda \tag{3}$$

where $f_{jk}(\lambda)$ measures the process covariance at frequency λ. The coefficient

$$\rho_{jk}(\lambda) = \frac{f_{jk}(\lambda)}{\sqrt{f_{jj}(\lambda) f_{kk}(\lambda)}}, 0 \le \rho_{jk} \le 1 \tag{4}$$

is known as the spectral coherence between Y_j and Y_k. Complete linear association of the two signals at the frequency λ holds when $\rho_{jk}(\lambda) = 1$, while $\rho_{jk}(\lambda) = 0$ indicates complete dissociation. The spectral lead of $Y_j(t)$ over $Y_k(t)$ at frequency λ is estimated as

$$\theta_{jk}(\lambda) = \operatorname{atan}\left(\frac{\operatorname{Im}(f_{jk}(\lambda))}{\operatorname{Re}(f_{jk}(\lambda))}\right) \tag{5}$$

where Re(.) and Im(.) denote real and imaginary part, respectively. Note that – up to a normalization factor – the partial correlations used by Cordes et al. (2001) are the real part η of the complex coherence

$$\eta_{jk}(\lambda) = \rho_{jk}(\lambda)\cos(\theta_{jk}(\lambda)) \tag{6}$$

In order to get robust estimators of (ρ,θ), we use the Parzen lag window method as suggested by Müller et al. (2001).

A procedure for the detection of resting-state networks

Following spectral coherence analysis, a difficult task consists in finding a simplified model of the pairwise interactions. In Müller et al. (2001), a direct thresholding is applied to the coherence matrix, and the set of mutually coherent voxel time courses are displayed. Besides the effect of more or less arbitrary thresholds, this does not handle the detection of multiple networks appropriately. In Cordes et al. (2002) a single-link hierarchical clustering technique was proposed, based on a pseudo-distance derived from partial correlation. However, such deterministic methods are sensitive to noise; they may yield inconsistent clusters (Stanberry et al., 2003) and require a lot of post hoc cluster validation. Lastly, they do not cope with the selection of the number of clusters better than standard methods.

To avoid these shortcomings, we turn to multivariate analysis, and introduce low-dimensional representations of the datasets based on the coherence matrix. These representations are intrinsically interesting since they give a geometrical representation of the global signal structure. Low-dimensional data can then be clustered more robustly and efficiently, using e.g. Gaussian Mixture Models (GMM) or C-means. Information criteria (e.g. BIC) provide then a data-tailored number q of clusters. These clusters can be interpreted as coherent modes of the dataset. If q is not too large, visual screening becomes an adapted exploration and validation procedure.

In what follows, we start by describing the datasets of our study. Then we develop the analysis procedure based on spectral coherence analysis suggested above. As in previous contributions on resting-state data analysis, we have not performed simulations of resting-state activity, since we have no real prior to build meaningful simulations. We show in the Results section that the networks found are interpretable in the view of neuroimaging literature, and discuss the inter-subject variability.

Materials and methods

Datasets and pre-processing

Data were acquired using a Bruker 3 T System at MRI Center of La Timone, Marseille. For datasets 1 to 3, 1524 volumes of 6 contiguous slices were acquired (TR = 303 ms) on three different subjects. Although cardiac and respiratory measures were performed simultaneously (Dodel et al., 2004), we do not use these information here. Datasets 4 to 9 were recorded on the same three subjects (sessions 4–5, 6–7 and 8–9 from subjects 1, 2 and 3, respectively), with more conventional acquisition parameters: 254 volumes of 36 slices were acquired (TR = 1813 ms; field of view 192 × 192 mm, matrix 64 × 64). Noticeably, the cardiac (and maybe respiratory) rate was aliased in the latter case, and not in the former case. However, complete brain acquisitions may benefit to the detection of spatially distributed activity networks. High resolution ($1 \times 1 \times 1$ mm^3) anatomical images were acquired for all subjects.

All the datasets were corrected for motion and delay in slice acquisition using the SPM2 (http://www.fil.ion.ucl.ac.uk/spm/software/spm2/) software. A mask containing only brain voxels was generated by thresholding mean functional images. After discarding the first scans, the number of available time points was $T = 1480$ for the first three sessions, and $T = 250$ for the others. The time courses were regressed against motion estimates in order to remove motion confounds, which have much impact in the low frequency band.

Analysis of the datasets

Fig. 1 summarizes the different processing steps of the data. The datasets are first reduced through a spatial under-sampling procedure: an intra-session parcellation algorithm (Thirion et al., in press) groups neighboring voxels with similar time courses. For the sake of place, the parcellation algorithm will not be detailed in this technical note. Whatever the method used (Flandin et al., 2002; Thirion et al., in press), the algorithm is assumed to cluster the data into spatially and functionally homogeneous units. Assuming that the signal of interest is spatially correlated, one expects that parcellation simplifies the dataset with minimal perturbation on the RSA structure. This method is less arbitrary than a pre-selection of voxels, and might reduce uncorrelated spatial noise. The resulting data matrix Y has a size $N \times T$, N being the number of parcels (here, 10^3) and T the number of time points.

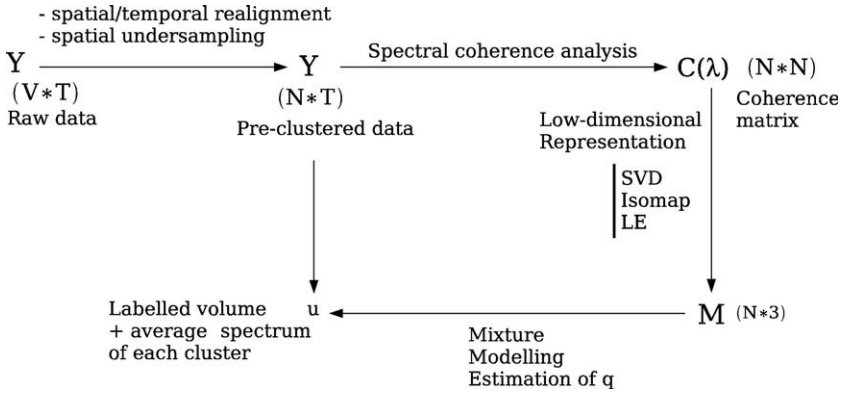

Fig. 1. List of procedures applied to the data, and variable names associated with them. After standard spatial and temporal realignment, the datasets are parcelled (spatial undersampling). Average spectral coherence is computed between all pairs of regions; a low-dimensional representation of the resulting coherence matrix is then derived using different techniques. Mixture modeling allows to identify homogeneous regions within the representation. The spectral characteristics of the cluster-wise average signals can then be further studied.

Spectral coherence analysis is then performed as follows: for all pairs of regions $(i, j) \in [1,\ldots,N]^2$, the coherence $\rho_{i,j}(\lambda)$ is computed for $\lambda = 0.02$ to $\lambda = 0.1$ Hz using a 0.02 Hz step, and the ensuing average coherence is derived. The matrix $\Omega = (\rho_{ij})$ of pairwise average coherences is then processed in order to get geometric representations of the coherence structure. Among the many available methods, we use either (a) a Principal Components Analysis of the centered coherence matrix, or nonlinear methods, like (b) Isomap and (c) Laplacian embedding (LE).

(a) Principal Components Analysis of the centered coherence matrix is given by

$$USV' = \mathrm{SVD}\left(\left(I_N - \frac{1}{N}J\right)\Omega\left(I_N - \frac{1}{N}J\right)\right) \quad (7)$$

where U, V are $N \times N$ orthogonal matrices, S a diagonal matrix, I_N the $N \times N$ identity matrix, and J the $N \times N$ matrix filled with ones; SVD stands for the Singular Value Decomposition. The centering is necessary because Ω contains only positive values. Moreover, this is a classical step in exploratory data analysis, when the *data center* has no particular importance. The p-dimensional representation M_p is then $M_p = (US)_p$, where $(.)_p$ denotes the reduction to the p first columns of this matrix.

Isomap and LE first proceed by forming the symmetric k-nearest neighbor graph G_k of the data endowed with the metric derived from spectral coherence, i.e. neighborhood is defined according to the highest mutual coherence.

(b) Isomap (Tenenbaum et al., 2000) is based on computing local distances and expanding them geodesically throughout the graph. The distances are initialized as

$$d_{ij} = \begin{cases} \sqrt{1-\rho_{ij}} & \text{if } (i,j) \text{ are } k-\text{neighbors} \\ \infty & \text{otherwise} \end{cases} \quad (8)$$

The resulting pairwise geodesic distance matrix Δ is derived using N repetitions of Dijkstra's algorithm, and is then analyzed through multidimensional scaling: again, we get Eq. (7), where Ω is replaced by Δ. The representation M_p is derived similarly from the first p components of the SVD.

(c) On the other hand, the LE method (Belkin and Niyogi, 2003; Thirion and Faugeras, 2004) is directly based on the adjacency matrix W^k of the graph G_k. The low-dimensional embedding is defined as the eigenfunctions of the normalized Laplacian L^k of W^k associated with its lowest eigenvalues; these functions can be thought of as the smoothest functions defined on the graph.

$$L^k_{ij} = \begin{cases} -W^k_{ij} \Big/ \sqrt{\left(\Sigma_l W^k_{il}\right)\left(\Sigma_m W^k_{jm}\right)} & \text{if } ij \\ 0 & \text{if } i = j \end{cases} \quad (9)$$

Here, we choose $k = 10$ and $p = 3$ in our implementation. While the outcome is not very sensitive with respect to k, the choice of a small value of p enables visualization, and prevents the ensuing GMM from being trapped into local maxima—which is advantageous for reproducibility. The GMM is applied, with the number q of clusters being defined through a Bayesian Information Criterion (BIC). Once the final clusters are obtained, the averaged time courses and their Fourier spectra are estimated for further characterization.

Assessment of the resulting clusters

Note that our procedures (initial clustering, dimension reduction, final clustering) induce progressive simplifications of the overall information; for instance, the number q of final clusters is systematically less than 10. This allows for a fast screening of the results.

For display, we select the clusters that have a *plausible* spatial layout, i.e. the clusters that are mainly in the grey matter, and that are not concentrated around vessels. According to the sessions, this represents one to four clusters. We also present the Fourier spectra of the corresponding cluster-averaged time courses, together with the average spectrum of the other time courses, in the band of interest [0 0.12] Hz. This semi-quantitative approach gets around the difficulty of using a quantitative criterion that adapts to different subjects and spatio-temporal configurations.

Results

We first compare the three representation methods. Then, we detail the results obtained with the LE representation method across sessions.

Comparison of the different representation methods

In Fig. 2, we show the output of the three representation techniques on one dataset: for each representation technique, a scatter plot of the first two coordinates $(M_1(n), M_2(n))$ is presented,

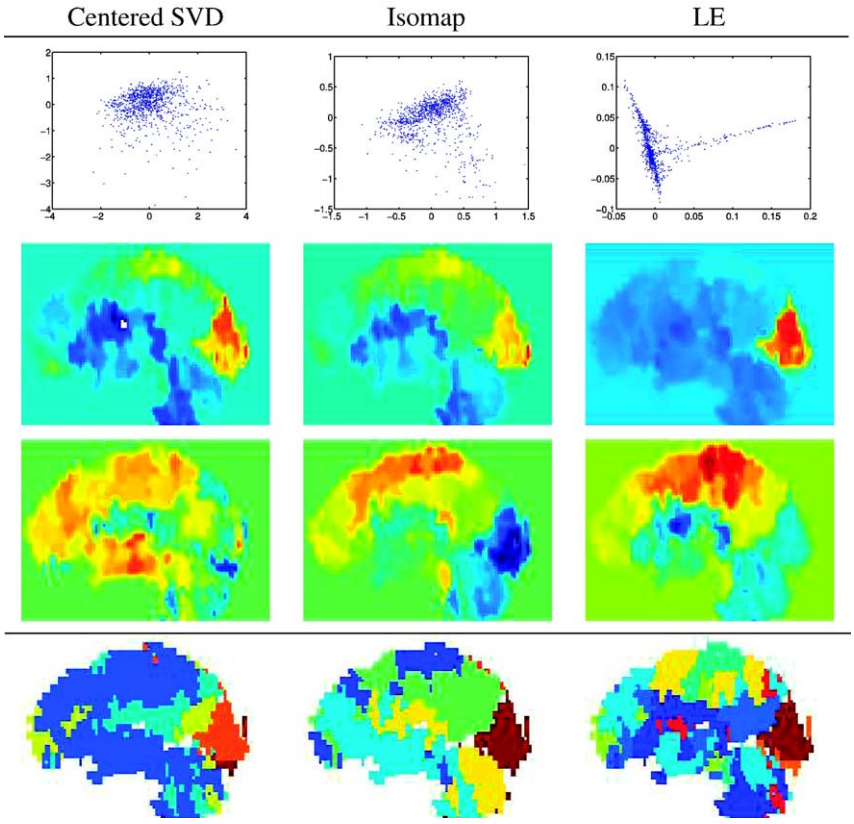

Fig. 2. Comparison of the three representation techniques used to analyze the coherence matrix: centered SVD, Isomap and Laplacian Embedding (LE). For either technique, a scatter plot of the first two coordinates ($M_1(n)$, $M_2(n)$) is presented (top), together with the corresponding spatial maps (middle), and clusters obtained with post-hoc GMM (bottom).

together with the corresponding spatial maps. The clusters obtained with post-hoc GMM are also presented.

It appears that the three methods yield comparable maps and clusters, though the linear method yields the least structured representation, while the LE yields a clearer picture of the coherence interactions. Not surprisingly, the LE representation yields more clusters, which are, however, very well structured anatomically – they match very nicely the boundaries between frontal, parietal, occipital areas and cerebellum – showing thus anatomically plausible RSA networks. Isomap yields a trade-off, i.e. an intermediate number of clusters (and thus an intermediate level of detail). This observation was quite general across the nine datasets analyzed (data not shown). Thereafter, we keep the representations derived by LE.

Description of the resting-state networks

Rapid acquisition scheme

The analysis of the short-TR datasets (datasets 1–3) is presented in Fig. 3. It reveals that an occipital cluster is visible in three cases, whose spatial homogeneity is less evident however in dataset 3. In dataset 2, the occipital network is divided into symmetric sub-clusters that delineate known visual areas (striate vs. extrastriate, and central vs. more peripheric areas).

Slow acquisition scheme

The analysis of the other datasets is presented in Figs. 4–6 for the three subjects, with two sessions in each case. Across sessions, the spatial reproducibility of RSA networks is strong: subject 1 has two occipital components and one or two parieto-frontal RSA clusters; subject 2 has two reproducible parieto-frontal components; subject 3 has a frontal cluster in both cases, and an occipital cluster in one session. The between-subject variability in the resulting networks is not negligible, and possibly larger than usually described in the literature (Kiviniemi et al., 2003). Moreover, the interpretation of some clusters, e.g. those of subject 3, is still under assessment. However, occipital and frontal clusters are consistently found in each subject. Most of the clusters are symmetric. These characteristics are strong indications of biologically relevant networks.

We have presented the spectra of the cluster-averaged time courses, together with the average spectrum of the other clusters. As already reported by Cordes et al. (2001) and Kiviniemi et al. (2003), these spectra clearly show an increase of power in the 0.02–0.03 frequency range for subject 1 (Fig. 4), while this increase is less pronounced for the two other subjects (Figs. 5 and 6).

We have also performed the analysis of these datasets based on the real part η of the complex coherence instead of ρ (cf. Eq. (6)), and obtained similar results (not shown).

Discussion

Technical aspects

We proposed a self-contained framework for the detection of RSA networks, based on the derivation of representations of the

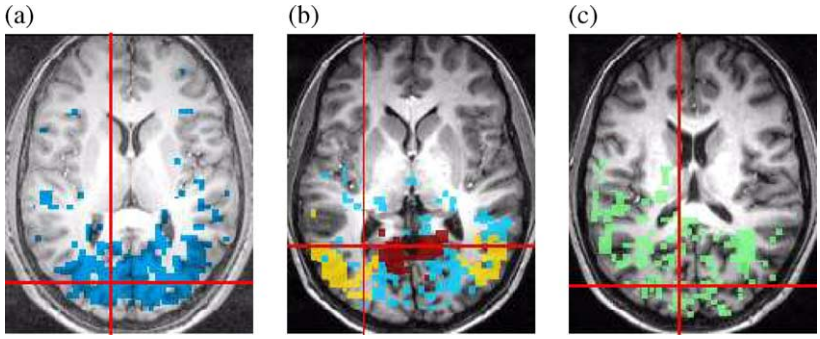

Fig. 3. Resting-state networks obtained from datasets 1 (a), 2 (b) and 3 (c) (partial brain acquisition): the anatomically most plausible clusters are represented. They are occipital in all three cases.

coherence matrix, that could reproducibly detect spatially plausible networks in three subjects. Note that correlation-based analysis on these datasets had been confounded by the physiological (motion, heart, respiratory) signals, and had not been able to report such networks (Dodel et al., 2004) as clearly. Coherence analysis concentrates on a frequency band ([0.01 0.1] Hz), where the impact of physiology is mild, and RSA known to be noticeable. Moreover, coherence, unlike correlation, is not affected by systematic time shifts in RSA.

Our detection procedure is data-driven, in the sense that we do not bias the detection towards pre-defined targets (*seed voxels* or ROIs); rather, we exploit the multivariate nature of the signals to find intrinsic structures. A key assumption is that the information embedded in the large coherence matrix can be well represented in a smaller dimensional space. In this space, clustering can segment the data into easily interpretable networks, while it could not perform as well in the original space. While this idea has been used e.g. in DT-MRI analysis (Brun et al., 2003) or protein structure analysis (Weston et al., 2004), it had not been previously described in the fMRI literature (although it was partly suggested in Thirion and Faugeras, 2004).

Among the possible methods, the Laplacian Embedding (LE) technique yielded particularly good results. More precisely, the first three components of the LE seem to contain more information than the first components of the other representation techniques. This is surprising, since, unlike the other methods, it induces clear metric distortions in the representation (see Eq. (9)), and does not take global metric information into account, as e.g. Isomap does. A possible interpretation is that the exact metric representation of the dataset is less important here than the representation of local interactions – spectral coherences – between different regions. The mixture model adopted for the final representation of RSA networks is less sensitive to noise and outliers than agglomerative clustering (Cordes et al., 2002), and allows for a reproducible selection of the number of clusters when used with the BIC.

An important step is the pre-clustering (parcellation) of the data into anatomically connected regions. Under the hypothesis that RSA is spatially correlated, this spatial undersampling procedure will not discard important information. Furthermore, it makes possible the computation and storage of wide interaction (here, coherence) matrices (see Thirion and Faugeras, 2003). It is also

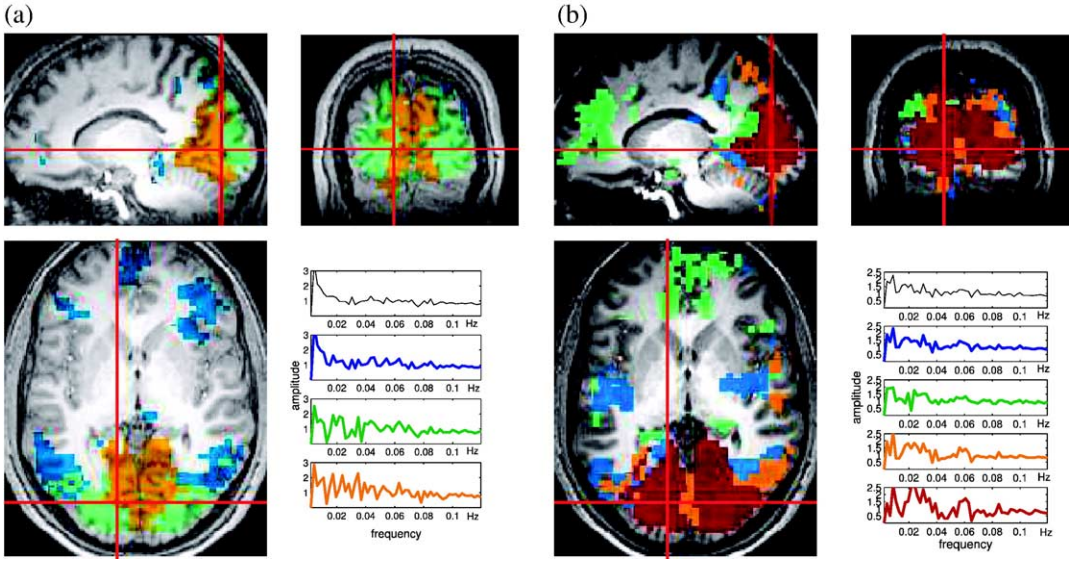

Fig. 4. Resting-state networks obtained from datasets 4 (a) and 5 (b) (subject 1, full brain acquisitions): the anatomically most plausible clusters are presented, together with the spectra of the cluster-averaged signals (same colors), and of the other time courses (black).

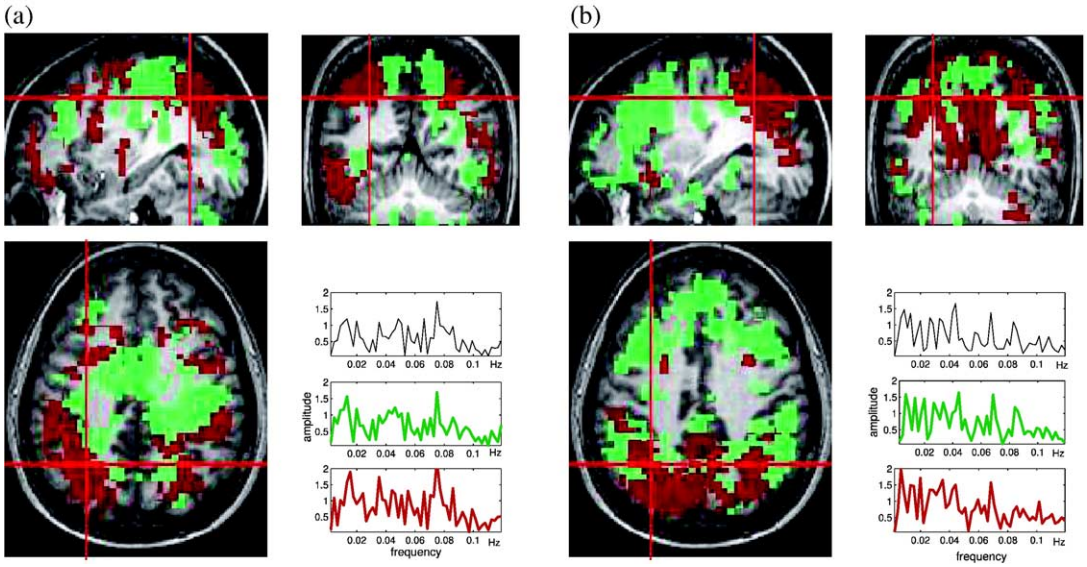

Fig. 5. Resting-state networks obtained from datasets 6 (a) and 7 (b) (subject 2, full brain acquisitions): the anatomically most plausible clusters are presented, together with the spectra of the cluster-averaged signals (same colors), and of the other time courses (black).

less arbitrary than selecting a subset of voxels based on their correlation with the other voxels (Cordes et al., 2002).

RSA networks

While intra-subject RSA clusters are clearly reproducible (see Figs. 4–6), inter-subject RSA clusters are more variable. Nevertheless, the occipital, parietal and parieto-frontal clusters have all been described previously, either in fMRI studies (Cordes et al., 2001), or in EEG-fMRI fusion studies (Goldman et al., 2002; Laufs et al., 2003). The definition and separation of the clusters are much easier in subject 1 (Fig. 4) than in the other subjects; in particular, the spectrum of the selected clusters shows the typical low-frequency contribution only in this case. This is probably attributable to different characteristics of the datasets in terms of contrast-to-noise ratio or motion, or it may be that our hypothesis on signal stationarity might not always hold. In particular, non-stationarity of the covariance structure may not be well accounted for by our band-pass filtering. One should also point out that RSA networks have no obvious definition, i.e. they depend on the state of the subject (a *resting state* is not a well-defined state). This motivates our choice to put more emphasis on intra-subject reproducibility, and on the similarity of the results after different processing strategies.

An interesting methodological question is whether rapid, but traditional acquisition schemes that allow only partial coverage of

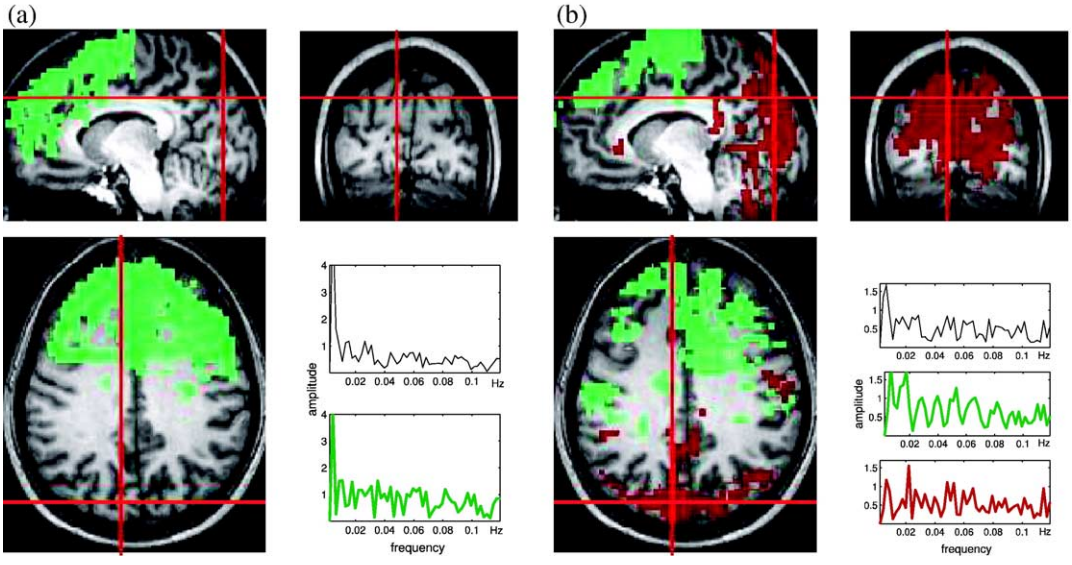

Fig. 6. Resting-state networks obtained from datasets 8 (a) and 9 (b) (subject 3, full brain acquisitions): the anatomically most plausible clusters are presented, together with the spectra of the cluster-averaged signals (same colors), and of the other time courses (black).

the brain should be preferred to slower acquisition scheme with full brain acquisition. Note that in the first case, due to the short TR (0.3 s), cardiac rhythm is not aliased, making spectral analysis more reliable, at the expense of reduced spatial information. To our knowledge, the present study is among the first that examine both cases. One can notice that the occipital component detected with the rapid acquisition scheme is particularly obvious on subject 1 (Fig. 3(a)). For this subject, occipital activity was also well detected with the slow acquisition scheme (Fig. 4). Given the variability of the RSA clusters obtained across subjects, we feel however that full brain acquisitions are more informative. The aliasing of cardiac rhythm in slow acquisition cases had probably a mild effect on the computation of spectral coherence in the frequency band used here ([0.01 0.1] Hz). Altogether, full brain acquisitions may be somewhat more attractive.

The nature of the networks that we describe can still be debated. In particular, the relative importance of vasomotion (Kiviniemi et al., 2003) and of the fluctuations of the resting state (Arieli et al., 1996) is still not clear. But the elucidation of this problem probably requires multimodal acquisitions.

Conclusion

In this paper, we presented a unified framework for the systematic study of Resting-State Activity (RSA) networks obtained in fMRI. It is based on several features, designed to handle the limitations of previous methods: (i) spatial reduction by a pre-clustering of neighboring voxels with similar time courses; (ii) spectral coherence analysis in the frequency band where RSA is known to be present ([0.01 0.1] Hz); (iii) a low-dimensional representation of the resulting coherence matrix, that retains the connectivity information. We found the Laplacian Embedding technique to be more sensitive; (iv) a Gaussian mixture model of the reduced data, in order to visualize the RSA networks. This procedure yielded reproducible results on a study with nine sessions, and seems to be powerful enough to adapt to cases where cardiac rhythm is aliased. We hope that these contributions will allow for a better understanding of the underlying processes, in particular in the case of simultaneous fMRI/EEG acquisition. Future work also includes the study of the effect of steady-state networks on activation patterns.

Acknowledgments

We thank Philippe Ciuciu and Andreas Kleinschmidt for their suggestions and help in the writing of this document, and Jean-Luc Anton for his contribution in data acquisition and analysis. This work was partly funded by the French ministry of research through concerted actions ‘masse de données’, ‘neurosciences intégratives et computationnelles’ and ‘connectivité’.

References

Arieli, A., Sterkin, A., Grinvald, A., Aertsen, A., 1996. Dynamic ongoing activity: explanation of the large variability in evoked cortical responses. Science 273 (5283), 1868–1871.

Beckmann, C., Smith, S., 2004. Probabilistic independent component analysis for functional magnetic resonance imaging. IEEE Trans. Med. Imag. 23 (2), 137–152.

Belkin, M., Niyogi, P., 2003. Laplacian eigenmaps for dimensionality reduction and data representation. Neural Comput. 15 (6), 1373–1396.

Biswal, B., Yetkin, F.Z., Haughton, V.M., Hyde, J.S., 1995. Functional connectivity in the motor cortex resting human brain using echo-planar MRI. Magn. Reson. Med. 34, 537–541.

Brun, A., Park, H.-J., Knutsson, H., Westin, C.-F., 2003. Coloring of dt-mri fiber traces using laplacian eigenmaps. Eurocast 2003, pp. 518–529.

Cordes, D., Haughton, V., Arfanakis, K., Carew, J., Turski, P., Moritz, C., Quigley, M., Meyerand, M., 2001. Frequencies contributing to functional connectivity in the cerebral cortex in “resting-state” data. AJNR Am. J.Neuroradiol. 22 (7), 1326–1333.

Cordes, D., Haughton, V., Arfanakis, K., Carew, J., Arfanakis, K., Maravilla, K., 2002. Hierarchical clustering to measure connectivity in fMRI resting-state data. Magn. Reson. Imaging 20 (4), 305–317.

Dodel, S., Poline, J.-B., Anton, J.-L., Brett, M., 2004. The influence of heartbeat and respiration on functional connectivity networks. Proc. 2th Proc. IEEE ISBI, pp. 380–383 (Arlington, VA).

Flandin, G., Kherif, F., Pennec, X., Malandain, G., Ayache, N., Poline, J.-B., 2002. Improved detection sensitivity of functional MRI data using a brain parcellation technique. Proc. 5th MICCAI, LNCS 2488 (Part I). Springer Verlag, Tokyo, Japan, pp. 467–474.

Friston, K.J., Frith, C.D., Liddle, P., Frackowiak, R.S.J., 1993. Functional connectivity: the principal-component analysis of large PET data sets. J. Cereb. Blood Flow Metab. 13, 5–14.

Goldman, R.I., Stern, J.M., Engel Jr., J., Cohen, M.S., 2002. Simultaneous EEG and fMRI of the alpha rhythm. NeuroReport 13 (18), 2487–2492.

Kiviniemi, V., Jauhiainen, J., Tervonen, O., Paakko, E., Vainionpaa, V., Rantala, H., Biswal, B., 2000. Slow vasomotor fluctuation in the fMRI of the anesthetized child brain. Magn. Reson. Med. 44, 378–383.

Kiviniemi, V., Kantolaa, J.-H., Jauhiainen, J., Hyvrinen, A., Tervonen, O., 2003. Independent component analysis of nondeterministic fMRI signal sources. Neuroimage 9 (2), 253–260.

Kiviniemi, V., Kantolaa, J.-H., Jauhiainen, J., Tervonen, O., 2004. Comparison of methods for detecting nondeterministic BOLD fluctuation in fMRI. Magn. Reson. Imaging 22 (2), 197–203.

Laufs, H., Krakow, K., Sterzer, P., Eger, E., Beyerle, A., Salek-Haddadi, A., Klienshmidt, A., 2003. Electroencephalographic signatures of attentional and cognitive default modes in spontaneous brain activity fluctuations at rest. Proc. Natl. Acad. Sci. U. S. A. 100 (19), 11053–11058.

Müller, K., Lohmann, G., Bosch, V., von Cramon, D., 2001. On multivariate spectral analysis of fMRI time series. Neuroimage 14 (2), 347–356.

Stanberry, L., Nandy, R., Cordes, D., 2003. Cluster Analysis of fMRI data using dendrogram sharpening. Hum. Brain Mapp. 20 (4), 201–219.

Sun, F.T., Miller, L.M., D’Esposito, M., 2004. Measuring interregional functional connectivity using coherence and partial coherence analysis of fMRI data. Neuroimage 21 (2), 647–658.

Tenenbaum, J., de Silva, V., Langford, J.C., 2000. A global geometric framework for nonlinear dimensionality reduction. Science 290, 2319–2323.

Thirion, B., Faugeras, O., 2003. Dynamical components analysis of fMRI data through kernel PCA. Neuroimage 20 (1), 34–49.

Thirion, B., Faugeras, O., 2004. Nonlinear dimension reduction of fMRI data: the Laplacian embedding approach. Proc. 2st Proc. IEEE ISBI, pp. 372–375 (Arlington).

Thirion, B., Flandin, G., Pinel, P., Poline, J.-B., in press. Dealing with the shortcomings of spatial normalization: multi-subject parcellation of fMRI data sets. Human Brain Mapping.

van de Ven, V.G., Formisano, E., Prvulovic, D., Roeder, C.H., Linden, D.E.J., 2004. Functional connectivity as revealed by spatial independent component analysis of fMRI measurements during rest. Hum. Brain Mapp. 22 (3), 165–178.

Weston, J., Elisseeff, A., Zhou, D., Leslie, C.S., Noble, W.S., 2004. Protein ranking: from local to global structure in the protein similarity network. Proc. Natl. Acad. Sci. U. S. A. 101 (17), 6559–6563.